

A correlation between the equilibrium and transport properties of intercalation systems.

E.V. Vakarin and J.P. Badiali

Laboratoire de Electrochimie et Chimie Analytique

ENSCP-UPMC, 11 rue P. et M. Curie, 75231 Cedex 05, Paris, France

Employing the lattice gas model, combined with the linear elasticity theory, a correlation between the equilibrium and transport properties of intercalated species is investigated. It is shown that the major features of the intercalation isotherms and the concentration dependence of the chemical diffusion coefficient can be well understood in terms of the change of the host volume in the course of intercalation. Theoretical predictions are compared to the experimental observations on PDH_x , Li_xWO_3 and Li-graphite systems.

PACS numbers: 68.35.Ct, 68.35.Rh

I. INTRODUCTION

Intercalation processes and their application in many technologically important domains, such as the design of hydrogen-storage systems [1], rechargeable high-energy batteries, electrochromic devices, (see Ref. [2] for a review), and superconductors [3].

The insertion process can be viewed (at least, in some aspects) as an adsorption of guest particles on the host lattice. For charged particles the ionic charge inside the matrix is compensated by the electrons. For that reason the electrochemical intercalation is also similar to a three-dimensional adsorption of neutral species. Based on this analogy the intercalation is traditionally described within the lattice gas (LG) model. In this approach all the properties (intercalation isotherm or capacity-concentration dependence) are connected with an ordering the guest on different adsorption sites of a rigid host lattice – the configurational transitions.

However, the host response to the accommodation of the guest species is not negligible. For instance, the insertion induces the stress into the host matrix. This may lead to segregation effects [4] or even to instabilities [5] of the host-guest system. Also a loading path is shown [6] to influence the guest uptake efficiency. Due to this the host may undergo an expansion or local distortion. Typical examples are the hydrogen sorption by metals [6,9], or the intercalation of Li ions into layered materials [10,13]. Quite often the host undergoes structural transformations [14,17] due to intercalation. These are the structural transitions. In such cases the standard LG approach also operates with several sublattices [10,17] corresponding to each conformation of the host. However, such a restructuring suggests that the elastic effects should be taken into account. A general thermomechanical theory of the stress-composition interaction is developed by Larche and Cahn [18]. This implies the existence of a coupling between

the elastic properties of the host material and the structure and/or the dynamics associated with the guest species. In other words the configurational and structural transitions should be considered to be coupled. In our previous papers we have investigated such a coupling for two-dimensional [19] as well as for three-dimensional systems [20,22]. The main advantage of our approach is its capability in describing various (microscopically different) intercalation systems within a common framework. Despite of the fact that some microscopic details are omitted, the theory agrees well with experimental data on layered Li_xTiS_2 and crystalline Li_xWO_3 and Na_xWO_3 compounds at equilibrium conditions.

In this study we focus on a correlation between the equilibrium properties (isotherms and differential capacity) and the concentration dependence of the chemical diffusion coefficient. Our purpose is to determine the impact of the thermodynamics to the kinetic properties. Following our previous works we combine the LG model, describing the configurational transitions and the linear elasticity theory that accounts for the loading mechanism and the volume dilatation in the course of the structural transitions (expansion or restructuring). This allows us to derive an effective chemical potential, involving the concentration dependent stress and strain fields. Then, assuming that the diffusion flux is proportional to the gradient of the chemical potential, we investigate the behavior of the chemical diffusion coefficient.

II. MODEL

A. Microscopic formulation

The host material is described as a three-dimensional lattice of adsorbing sites with their positions given by a set vectors (\mathbf{r}_i) . Due to the elastic properties of the real host each site (for instance, an interstitial site) of this "auxil-

lattice may deviate from its equilibrium position r_i^0 , such that we deal with the displacements $u_i = r_i - r_i^0$. Therefore, the host properties are described by the Hamiltonian $H_H [fu_i]$. Note however that a connection between the elastic properties of the matrix and those of the adsorbing lattice, is not straightforward [20,21].

A distribution of the intercalants on the host sites is given by a set of occupation numbers ft_{ij} , with $t_i = 0$ or $t_i = 1$. The guest subsystem is characterized by the chemical potential and the nearest neighbor interaction parameter W (at equilibrium positions). For the electrochemical insertion, chemical potential gives a deviation of the electrode potential eV from its standard value E_0 . In this way an arrangement of the intercalants on a rigid host lattice is governed by the LG Hamiltonian

$$H_G = W \sum_{ij} t_i t_j + \sum_i \epsilon_i t_i \quad (1)$$

that describes the configurational transitions of the intercalated species. These could be the droplet formation for attractive interactions ($W < 0$) or the order-disorder transition for repulsive interactions ($W > 0$). In the latter case one introduces the sublattice concentrations as appropriate for the symmetry of a given system.

The coupling between the host and the guest is given by Hamiltonian $H_C [fu_i; ft_{ij}]$ which takes into account a dependence of the binding energy on the site displacement and also the pairwise interaction between the guest particles through the host lattice. The overall Hamiltonian is now written as

$$H = H_H [fu_i] + H_G [ft_{ij}] + H_C [fu_i; ft_{ij}] \quad (2)$$

The free energy F corresponding to the above Hamiltonian is given by

$$F = F_H + F_G(x) + F_C(x) \quad (3)$$

where x is the intercalant concentration. Here F_H is the host free energy in the absence of intercalation, F_G is the guest free energy in a case of the rigid host lattice. The latter term can be calculated using the mean field approximation to obtain the well-known relation [2,10] for the chemical potential

$$\mu_0(x) = eV - E_0 = cWx + \frac{1}{1-x} \ln \frac{x}{1-x} \quad (4)$$

where c is the coordination number of the host lattice and $\beta = 1/kT$. The coupling term $F_C = -\ln(\text{tr} e^{\beta H_C})$ requires the averaging over the displacements and the occupation numbers, calculated with the reference terms H_H and H_G . In fact, this is an infinite series including the

correlations of all orders in the reference state. The main problem is to specify $H_C [fu_i; ft_{ij}]$ coherently with the host symmetry and elastic properties. It is known that real host materials have rather complicated elastic properties (e.g. a strong anisotropy). Therefore, only some simplified model calculations are expected to give tractable results. On the other hand, such predictions (e.g. a rigid plane model [23]) do not exhibit quantitative agreement with experimental data.

B. Approximation

The perturbative scheme developed previously [20,21] has shown that the coupling term is concerned with a concentration dependence of the host response to the intercalation. This involves at least two effects. First is a renormalization [2,24] of the net pair interaction between the intercalants due to their indirect interaction through the matrix. The second is a change of the host volume upon insertion of the guest species. Depending on the host nature, a stress field may result if the lattice is not totally free to relax. In this situation it seems reasonable to estimate the coupling term based on the continuum theory of elasticity with the concentration dependent stress and strain fields. Then the host-guest free energy is a sum of the lattice gas and elastic part

$$F(x) = F_{LG}(x) + F_{el}(x) \quad (5)$$

where $F_{LG}(x)$ is the configurational (lattice gas) part, in which the pairwise interaction is renormalized [2] due to the interaction through the matrix. This gives the chemical potential $\mu_0(x)$ (see eq. (4)) with a new interaction constant W . The elastic part is approximated by the free energy of a strained isotropic body under a loading stress $\sigma(x)$. Since the strain is assumed to be purely dilatational, we operate with traces and of the corresponding tensors.

$$F_{el}(x) = \frac{1}{2} \sigma(x)^2 \epsilon(x) \quad (6)$$

with ϵ being the effective elastic constant, independent of the concentration. The total stress $S = S(x)$ is given by

$$S(x) = \frac{dF_{el}}{d\epsilon(x)} = \sigma(x) \epsilon(x) \quad (7)$$

Therefore, we have two stress contributions. The internal, or self-stress $\sigma(x)$ corresponds to the host reaction to the guest insertion. The second term $\epsilon(x)$ describes a loading procedure, that may include the sample clamping or other effects which are not directly related to the strain. It is important that, in general, $\epsilon(x)$ is a function of x (not

a function of $\alpha(x)$). For instance, if the sample is clamped such that $\alpha(x) = 0$, then we have a stress accumulation proportional to the concentration $\alpha(x)/x$.

III. EQUILIBRIUM PROPERTIES

The guest chemical potential $\mu(x)$ is given by the concentration derivative of the total free energy.

$$\mu(x) = \mu_0(x) + S(x) \frac{d\alpha(x)}{dx} - \frac{d\alpha(x)}{dx} \alpha(x) \quad (8)$$

Here the second term involves the so-called chemical expansion coefficient $d\alpha(x)/dx$, while the last term is associated with the loading path. It is seen that the intercalation level depends on an interplay of the internal stress and the loading stress. The latter could be small, but its concentration derivative is not necessarily small, so that the loading path may induce serious consequences [6]. In particular, for a given material (α) and a suitable loading path $\alpha(x)$, there may be a cancellation of the last two terms in eq. (8) in a given domain of x . This explains why in some cases the purely configurational description $\mu(x) = \mu_0(x)$ works well.

For comparison to other theoretical approaches it is convenient to express the strain function in terms of other relevant quantities. The strain can be measured as a volume dilatation or as a change of the interlayer spacing in the course of insertion. If $V(x)$ is a composition dependent sample volume (or interlayer spacing for layered compounds), then by definition

$$\alpha(x) = \frac{V(x) - V(0)}{V(0)} = p(x) \quad (9)$$

where $\alpha = [V(x) - V(0)]/V(0)$ is the relative volume variation and $p(x) = [V(x) - V(0)]/[V(1) - V(0)]$ is a modulating function. The latter varies in between 0 and 1. If $p(x)$ is a linear function, then the system is said to obey the Vegard's law [25].

If the host-guest system forms a solid solution, then the guest partial molar volume $V_m(x)$ is related to the total volume

$$V(x) = xV_m(x) + V(0); \quad (10)$$

where $V(0)$ is the initial host volume (at $x = 0$). Then we can find the following relation for the strain, the volume variation and partial molar volume

$$\alpha(x) = \frac{V(x) - V(0)}{V(0)} = x \frac{V_m(x)}{V(0)} \quad (11)$$

If the loading is composition independent $\alpha(x) = \alpha_0$ and the sample volume changes linearly ($V_m =$

const ; $\alpha(x) = \alpha_0$), like in the PdH_x - phase), then we recover the well-known result [9]

$$\alpha(x) = \alpha_0(x) = x \frac{V_m}{V(0)} = \frac{V_m}{V(0)} \quad (12)$$

The term linear in the concentration can be viewed as an additional interaction which can be combined with dW/dx in $\mu_0(x)$. Although this additional term is proportional to the elastic constant, it is physically different from the interaction of elastic dipoles [2,24] which is already absorbed into W (see the discussion after equation (5)). This interaction takes place even if the sample is perfectly clamped ($\alpha(x) = 0$), while our term represents a cooperative effect due to $\alpha(x) \neq 0$.

In order to analyze the role of elastic effects in the phase behavior of the guest species it is instructive to consider a simple example of vanishing loading stress $\alpha(x) = 0$, $S(x) = \alpha(x)$. In this case there is no difference between the volume expansion or contraction. Then we arrive at

$$\mu(x) = \mu_0(x) + p(x) \frac{dp(x)}{dx} \quad (13)$$

where $\alpha = \alpha_0^2$. In addition, $p(x)$ is taken to be that in the so-called layer rigidity model [25] which describes a deviation from the Vegard's law in layered compounds

$$p(x) = 1 - (1 - x)^q \quad (14)$$

where q is related to the rigidity of the host layers. The first order phase transition (of liquid-gas type) is manifested by a singularity in the differential capacity $C = d\alpha/dx$

$$C = \frac{d\alpha_0(x)}{dx} + \frac{dp(x)}{dx}^2 + \frac{d^2p(x)}{dx^2} \quad (15)$$

It is clear that for $q < 1$ both derivatives of $p(x)$ are positive and the only possibility for the critical behavior is the case of attractive interactions $W < 0$, i.e. when the configurational part

$$\frac{d\alpha_0(x)}{dx} = \frac{1 + dW/dx(1 - x)}{x(1 - x)} \quad (16)$$

becomes negative. Then the last two terms in the denominator of (15) rescale the critical temperature and shift the critical composition from $x = 1/2$. For $q > 1$ the term d^2p/dx^2 becomes negative and the criticality may appear due to the elastic effects even if $W = 0$. The coexistence curves for this case, obtained by a numerical analysis of the divergence in C , are plotted in Fig. 1.

It is seen that the critical temperature (the maximum) increases with increasing q . Simultaneously the critical concentration decreases. The elastic effects break the hole-particle symmetry of the problem and consequently the curves are not symmetric and are not centered around $x = 1/2$.

In our previous works [20,22] we have analyzed another extreme case of vanishing total stress $S(x) \rightarrow 0$ and the loading stress proportional to the concentration $\sigma(x) = \sigma_0 x$. Then

$$p(x) = \sigma_0(x) + p(x) \quad (17)$$

where $\sigma_0 = \sigma_0$. Note, however that, for $\sigma = \text{const}$, the above result is valid only for a linear behavior of $p(x) = px$, while is an approximation for an arbitrary $p(x)$. In reality the elastic constants could depend on the concentration, for instance the bulk modulus of Pd is reduced [8] up to 20% due to the hydrogen sorption. Thus one can easily imagine a situation when $\sigma(x) \propto p(x)$ and then the approximation (17) is applicable for a nonlinear $p(x)$. In general, for a non-Vegard's behavior and the linear loading $\sigma(x) = \sigma_0 x$ we deal with

$$p(x) = \sigma_0(x) + p(x) + x \frac{dp(x)}{dx} \quad (18)$$

The strain can be measured as a volume dilatation or as a change of the interlayer spacing during the transitions between different phases (staging in graphite, restructuring in Li_xWO_3 , transition in PdH_x , etc). In any case the lattice parameters do not obey the linear Vegard's law [25], exhibiting a sharp change near the transition compositions x_n^0 . This can be described by the following approximation [20,22].

$$p(x) = \frac{1}{2} \left(1 + \sum_n p_n \tanh \left[\frac{x - x_n^0}{\Delta x_n} \right] \right) \quad (19)$$

where n counts the number of phase boundaries. In Li_xWO_3 , $n = 1; 2$ corresponds to monoclinic-tetragonal and tetragonal-cubic transitions, respectively. For Li-graphite systems, n corresponds to the stage transfer boundaries [12,13]. The set of rigidity parameters p_n controls a local slope and p_n are the weights corresponding to each phase, such that $\sum_n p_n = 1$. This is consistent with experimental observations [14] indicating that the structures are not completely pure, but contain some features that indicate a mixing of phases. The present form of $p(x)$ corresponds to continuous structural transitions, but can be easily modified to take into account the jump-like behavior (like for the staging [2]). Nevertheless, in that case the concentration derivatives of $p(x)$ would be singular, inducing the singularities in the thermodynamic quantities (as it should be in the neighborhood of a phase transition). Note however that the

experimental dependencies are usually smoothed due to a finite concentration resolution. Then it is difficult to distinguish between the step-wise variation and a sharp (but continuous) transition. For that reason the criticality criteria, determined on the ground of rigorous statistical mechanical arguments (loops or a divergent capacity $C(x)$), only approximately conform to experimental data. Therefore we stay with the continuous $p(x)$, performing the fitting to the experiment.

Following this methodology, in Fig. 3 we display the intercalation isotherm (inset) and the capacity curve, comparing them to the experimental data [14] for Li_xWO_3 . The fitting (eq. (18)) is performed assuming that the effective pair interaction inside the matrix is repulsive for any x . The curve modulation results from the strain behavior $p(x)$, associated with the volume dilatation. As is discussed previously [21,22], the peculiarities (inflection points and the peaks in $C(x) = dx/d(\mu)$) mark the boundary between different host symmetries. From the experimental point of view, the peak height is usually associated with a transition sharpness. Nevertheless, as we have discussed above, the critical behavior of the model itself should be studied separately.

IV. CHEMICAL DIFFUSION COEFFICIENT

In many cases there are two mobile species inside host matrices: the host electrons and the guest particles. Therefore, the transport is characterized by their flux densities J_e and J_G , related to the gradients of the corresponding chemical (or electrochemical) potentials μ_e and μ_G .

$$J_e = L_{ee} r_{\mu_e} + L_{eG} r_{\mu_G} \quad (20)$$

$$J_G = L_{GG} r_{\mu_G} + L_{Ge} r_{\mu_e} \quad (21)$$

where L_{ab} are phenomenological transport coefficients, which are scalar quantities if the host is spatially isotropic. In matrices with a metallic conductivity the electrons are much more mobile than the guest species. Due to this the guest ionic charge is compensated by the electrons. For the same reason the electrons reach a uniform (equilibrium) distribution much faster than the intercalants ($r_e = 0$ on the time scale when $r_G \neq 0$). In addition, usually $L_{GG} \gg L_{eG}$ [2]. Therefore one may focus on the guest flux

$$J = M(x) x r_{\mu_G} = D(x) r_{\mu_G} \quad (22)$$

where $M(x)$ is the mobility coefficient that must contain a blocking factor $M(x) = D_0(1-x)$, determining the concentration-dependent chemical (or collective) diffusion coefficient $D(x)$. A comprehensive review of theoretical approaches to the

determination of the chemical diffusion coefficient can be found in Ref. [26]. In the simplest approximation we deal with

$$D(x) = D_0(x)(1-x)\frac{d}{dx} = D_0(x)(1-x)C(x) \quad (23)$$

Under the assumptions above, the intercalant transport is described by the diffusion equation with an effective diffusion coefficient $D(x)$. The latter requires an information on the intercalation isotherm $C(x)$. Then, based on the equilibrium properties, at a given concentration gradient, one, at least in principle, can solve the kinetic problem.

Note, that such a simple scheme should be modified when the host conductivity changes remarkably upon the intercalation. Then the electronic impact should be taken into account. Also, we do not consider other driving forces, like external field or stress gradients, assuming that the guest concentration, x , is the only independent variable. And finally, near the phase coexistence (e.g., staging) a system becomes non-uniform because of the phase boundaries. Then the formulation of the kinetic problem must be coherent with the theory of critical phenomena (see [30] for a recent review).

Starting from (8) and (23) we obtain

$$D(x) = D_0(x) + D_{el}(x) \quad (24)$$

where the first term is the standard LG part $D_0(x) = D_0(x)(1-x)\frac{d}{dx}$ and the elastic contribution is given by

$$D_{el} = B(x) \left[\frac{d^2}{dx^2} + \frac{d}{dx} \left(2 \frac{d}{dx} \frac{d}{dx} \right) \frac{d^2}{dx^2} \right] \quad (25)$$

with $B(x) = D_0(x)(1-x)$. The diffusion coefficient involves several competing factors (strains, stresses and their concentration derivatives). In general it is not trivial to see whether D increases or decreases with x . The situation is even more complicated for systems in which the lattice spacing does not obey the linear Vegard's law, but has inflection points separating different phases (e.g., staging in graphite or restructuring in Li_xWO_3). Then the derivatives above may change sign with the concentration. Also we see again that the badging path has a significant contribution.

For PdH_x (β -phase) we recover the well known result [8,9]. The concentration induced internal stress $S_0(x) = xV_m/V_0$ increases the diffusion

$$D = D_0(x) + B(x) \frac{V_m^2}{V_0}; \quad (26)$$

where $D_0(x)$ is the stress free contribution (it corresponds to $D_0(x)$, i.e. the lattice gas description, see above). Note that the non-local stress effects [7,8] are not discussed here.

Since, according to (23), the diffusion coefficient is just an inverse of $C(x)$, D as a function of x has a minimum (Fig. 3), corresponding to the peaks in the capacity curve. For WO_3 (Fig. 3) the theory works well near the first minimum, but overestimates the diffusion at higher x . Assuming that eq.(23) is valid, we have also inverted the capacity data (Fig. 2) in order to demonstrate that there is no "hidden" errors in the fit for $C(x)$. Since the equilibrium characteristics (Fig. 2) are predicted with a reasonable accuracy, then one of the sources for the discrepancy could be our simplified assumptions on the mobility. For instance, one might suppose that eq.(23) does not work for higher x because the hopping D_0 depends on the elastic properties. By the analogy with the two-dimensional diffusion [26], D_0 is related to the lattice spacing. The latter decreases with x for WO_3 [15], so that the resulting $D(x)$ would also decrease. Nevertheless the volume change does not exceed several percents [2,15]. This cannot explain the two orders of magnitude difference in Fig. 3. The lattice anisotropy seems also to be irrelevant because the final (high x) structure is cubic, so the isotropic approximation for the diffusion and elastic properties is reasonable.

It is known [27] that Li_xWO_3 changes its electronic conductivity near the structural instability composition. Then the ionic transport must correlate with the transport of the neutralizing electrons. Similar effects occur in superconductors [3]. Therefore, the electronic mobility impact (that is absent from our approach) to the current should be taken into account by including the additional driving force $r_e = d_e/dx \cdot x$. This contribution can be included into our approach, assuming some model for the electronic structure, e.g. - the rigid band model. This would correct our predictions for small x (according to [27], for $x \rightarrow 0$), but our high- x estimation would remain unchanged. We believe that the electronic effects are not responsible for the decrease of $D(x)$ at high concentrations. Based on the fact [27] that the electrical properties of Li_xWO_3 become more and more metallic with increasing Li content, we may expect that our approximation $r_e = 0$ becomes more reliable with increasing x . Moreover, if the conductivity effects were important, then the ionic diffusion would increase like this occurs in amorphous WO_3 [28].

In our opinion we deal with an interplay of several facts. Although the model works well in predicting the equilibrium properties, nevertheless it is probably too simple for the description of the kinetics. In fact, the transport is assumed to take place in an infinite lattice through the hopping of neutral species ($\text{Li}^+ + e$), ignoring the kinetics of other relevant phenomena, like the charge transfer (metal/host, guest/host), the exclusion (perm se-

lectivity) effect [20], the formation of the passive layer at the host/electrolyte boundary, etc. On the other hand, the experimental data on the diffusion are extracted from direct measurements employing a theoretical model, which could differ (in some details) from the one introduced here. Concerning the order of magnitude estimations, it should be noted that the experimental data for the same substance are usually differ significantly depending on the sample preparation, its size and the scanning time interval. Therefore, the quantitative description of the ionic transport is a delicate problem requiring mutual theoretical and experimental efforts. Nevertheless, our estimation of the elastic effects is qualitatively correct in predicting that the system characteristics changes coherently with the strain $p(x)$, and therefore, positions of the minima (Fig. 3) x_n^0 are predicted correctly, implying a correlation between the $D(x)$ behavior and the strain development.

Similar situation takes place for Li-graphite. In Fig. 4 the normalized interlayer spacing for graphite in the presence of intercalated Li is plotted as a function of the guest composition. The fitting is performed using eq. (19) under a suitable choice of the parameters p_n , α_n , x_n^0 . The experimental data are taken from Refs. [12,13]. Our fit is rather reasonable, "catching" the fact that the stage transfer compositions x_n^0 approximately correspond to the inflection points in $p(x)$, where the average interlayer spacing changes sharply. Note that we do not discuss the fine structure of the phase diagram [12], such as dilute and liquid-like phases for the same stage. These features are related to the guest in-plane ordering which is indistinguishable in the behavior of the interlayer spacing.

Having a reliable approximation for $p(x)$ we calculate the diffusion coefficient in the framework outlined above. The fitting to the experimental data [31] is shown in Fig. 5. It is seen that the diffusion slows down significantly near the stage transfer compositions x_n^0 . Although the magnitude of $D(x)$ is close to the experimental results, the width of the minima is underestimated. Note that the fitting is not optimized, that is, we did not try to find an optimal set of the parameters, which gives equally good agreement for the isotherm $p(x)$ and $D(x)$. Nevertheless, as in the case of Li_xWO_3 (Fig. 3), there is a clear correlation between the diffusivity and the strain behavior.

V. CONCLUSION

In summary, our approach implies that the main equilibrium and transport features of the intercalation systems (which differ in their microscopic details) can be well understood in terms of a concen-

tration dependence of the hydrostatic parts of the stress and strain fields, associated with the internal and loading effects [6]. It is shown that the elastic effects may induce the critical behavior even if the "direct" interaction between the guest species is absent. Although the ionic transport is supposed to be equivalent to the diffusion of neutral (ion plus electron) species, the approach is flexible enough to incorporate other transport mechanisms (migration, or electronic mobility effects).

The theory gives a quantitative description of different insertion processes, involving the volume expansion (Li_xTiS_2 (see [20]), P dH_x), staging (Li-graphite) or restructuring (Li_xWO_3). For all these processes the theory implies a correlation between the intercalation isotherm and a concentration dependence of the diffusion coefficient. The latter exhibit a set of characteristic minima, related to the boundaries between different phases (like different symmetry phases of Li_xWO_3 , transition in P dH_x , etc). However the experimental dependencies are usually smoothed due to a finite concentration resolution. For that reason the criticality criteria, determined on the ground of rigorous statistical mechanical arguments (e.g. $D(x) = 0$ at the transition concentrations) only approximately conform to the experimental data, exhibiting a sharp (but finite) decrease of D .

For a non-Vegard's strain variation the diffusion coefficient is a nonlinear (and nonmonotonic) function of the concentration (25). Therefore the diffusion equation for the concentration profile would be strongly nonlinear. Then one can expect a rather complicated space-time variation, including, for instance, oscillations [6] and other nonlinear effects.

Our results may have implication in various domains related to the insertion process, like hydrogen sorption [1], electrochemical intercalation, impurities in alloys, layered superconductors [3], volume transitions in hydrated gels [32], etc.

-
- [1] L. Schlappbach, A. Züttel, Nature 414, 353 (2001)
 - [2] W. R. McKinnon, R. R. Haering, in Modern aspects of Electrochemistry, edited by R. E. White, J. O'M. Bockris, and B. E. Conway (Plenum, NY, 1983), No 15, p 235
 - [3] J. S. Slusky et al, Nature 410, 343 (2001)
 - [4] C. A. Laberge, P. Fratzl, J. L. Lebowitz, Phys. Rev. Lett. 75, 4448 (1995)
 - [5] B. J. Spencer, P. W. Voorhees, J. Tersoff, Phys. Rev. Lett. 84, 2449 (2000)
 - [6] A. De Nino, V. Violante, A. La Barbera, Phys. Rev. B 56, 2417 (1997)

- [7] B. Baranowski, *J. Less-Common Metals*, 154, 329 (1989)
- [8] P. Zoltowski, *Electrochim. Acta*, 44, 4415 (1999)
- [9] W.-S. Zhang, X.-W. Zhang, Z.-L. Zhang, *Phys. Rev. B*, 62, 8884 (2000)
- [10] A. J. Berlinsky, W. G. Unruh, W. R. McKinnon, R. R. Haering, *Solid State Comm.* 31, 135 (1979)
- [11] A. H. Thompson, *Phys. Rev. Lett.* 40, 1511 (1978)
- [12] J. R. Dahn, *Phys. Rev. B* 44, 9170 (1991)
- [13] J. R. Dahn, F. Fong, M. J. Spoon, *Phys. Rev. B* 42, 6427 (1990)
- [14] M. Strömme Mattsson, *Phys. Rev. B* 58, 11015 (1998)
- [15] Q. Zhong, J. R. Dahn, K. Colbow, *Phys. Rev. B* 46, 2554 (1992)
- [16] Y. Gao, J. N. Reiners, J. R. Dahn, *Phys. Rev. B* 54, 3878 (1996)
- [17] T. Zheng, J. R. Dahn, *Phys. Rev. B* 56, 3800 (1997)
- [18] F. C. Larche, J. W. Cahn, *Acta Metall.* 33, 331 (1985)
- [19] E. V. Vakarín, A. E. Filippov, J. P. Badiali, *Phys. Rev. Lett.* 81, 3904 (1998)
- [20] E. V. Vakarín, J. P. Badiali, M. D. Levi, D. Aurbach, *Phys. Rev. B* 63 014304 (2001)
- [21] E. V. Vakarín, J. P. Badiali, *Electrochim. Acta* 46, 4151 (2001)
- [22] E. V. Vakarín, J. P. Badiali, *J. Phys. Chem. B* 106, 7721 (2002)
- [23] M. F. Thorpe, W. Jin, S. D. Mahanti, *Phys. Rev. B* 40, 10 294 (1989)
- [24] V. I. Kalimanov, S. W. de Leeuw, *J. Chem. Phys.* 116, 3083 (2002)
- [25] S. Lee, H. Miyazaki, S. D. Mahanti, S. A. Solin, *Phys. Rev. Lett.* 62, 3066 (1989)
- [26] R. Gomber, *Rep. Progr. Phys.* 53, 917 (1990)
- [27] J. Molenda, A. Kubik, *Solid State Ionics* 117, 57 (1999)
- [28] S. I. Pyun, J. S. Bae, *J. Alloys and Compounds* 245, L1 (1996)
- [29] M. Strömme Mattsson, *Solid State Ionics* 131, 261 (2000)
- [30] E. B. Nauman, D. Q. He, *Chem. Engineering Sci.* 56 (2001) 1999
- [31] M. D. Levi, D. Aurbach, *J. Phys. Chem. B* 101, 4641 (1997)
- [32] S. Sasaki, H. Maeda, *Phys. Rev. E* 54, 2761 (1996)

FIG. 1. Liquid-gas coexistence curves for the layer rigidity model in the absence of the direct interaction $W = 0$.

FIG. 2. Differential capacity and the voltage (inset) for crystalline Li_xWO_3 . The symbols correspond to the experimental data [12]. The parameters $p_1 = 0.7$, $p_2 = 0.3$, $\mu_1 = \mu_2 = 15$, $x_1^0 = 0.05$, $x_2^0 = 0.27$, $\mu = 1.8$, $\mu_0 = 0.01$, $W = 2.2$.

FIG. 3. The chemical diffusion coefficient for crystalline Li_xWO_3 . The symbols (up triangles) correspond to the experimental data [24]. The parameters are the same as for the previous figure.

FIG. 4. The average interlayer spacing for Li-graphite. The experimental data are extracted from [12,13]. The theoretical fitting is performed using equation (19), where $p_1 = 0.28$, $\mu_1 = 30$, $x_1^0 = 0.04$, $p_2 = 0.22$, $\mu_2 = 20$, $x_2^0 = 0.25$, $p_3 = 0.5$, $\mu_3 = 10$, $x_3^0 = 0.75$

FIG. 5. The chemical diffusion coefficient for Li-graphite. The experimental data are extracted from [31]. The fitting is done using equations (18) and (23) where $\mu W = 0.1$, $\mu = 0.5$, $\mu_0 = 0.1$

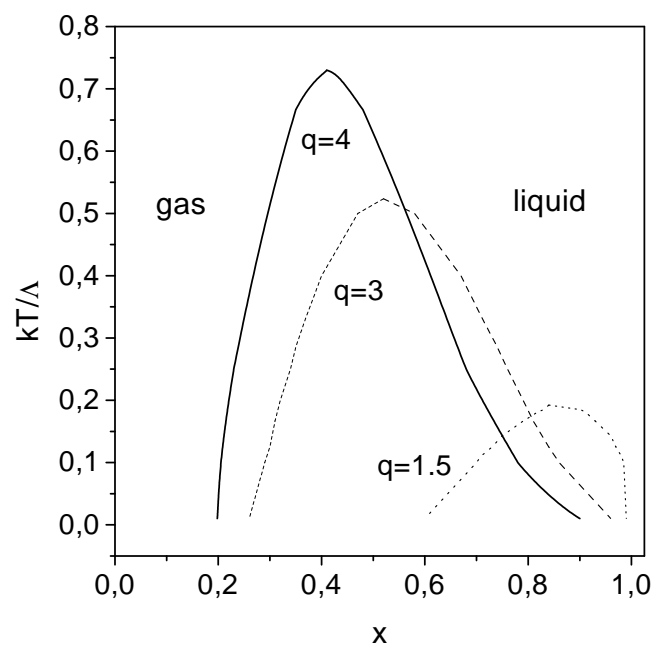


Figure 1

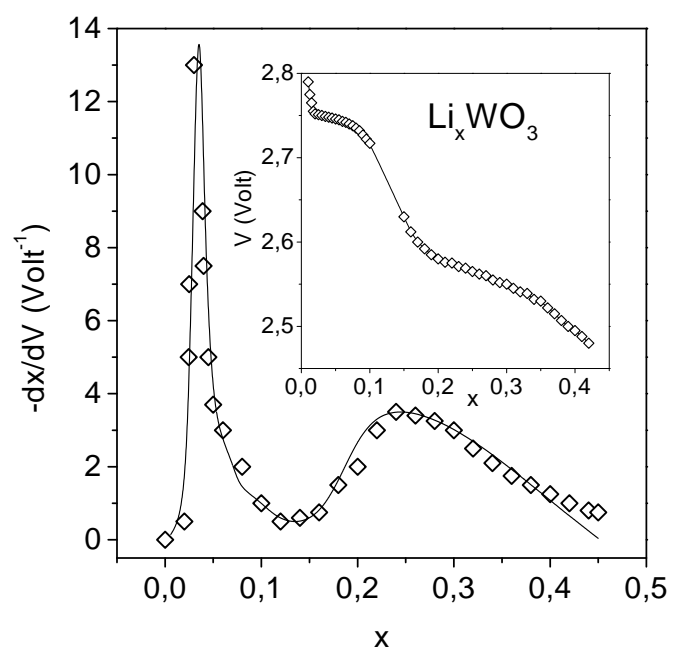


Figure 2

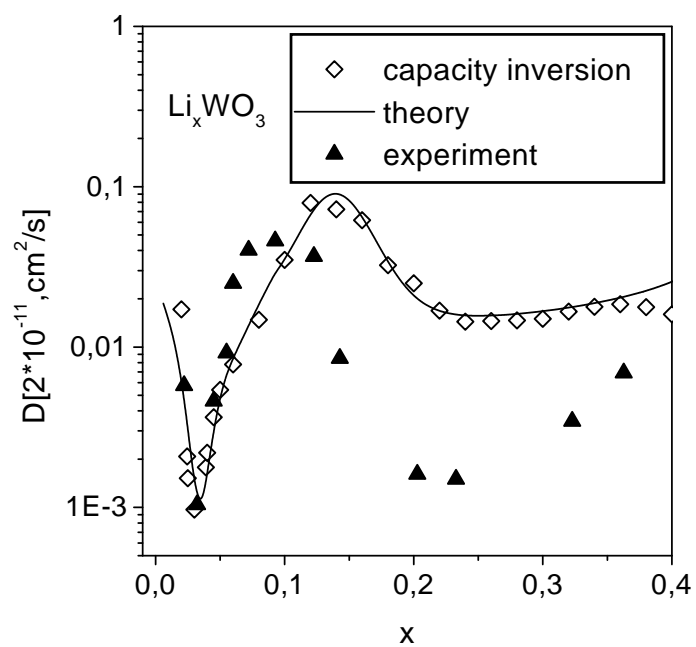


Figure 3

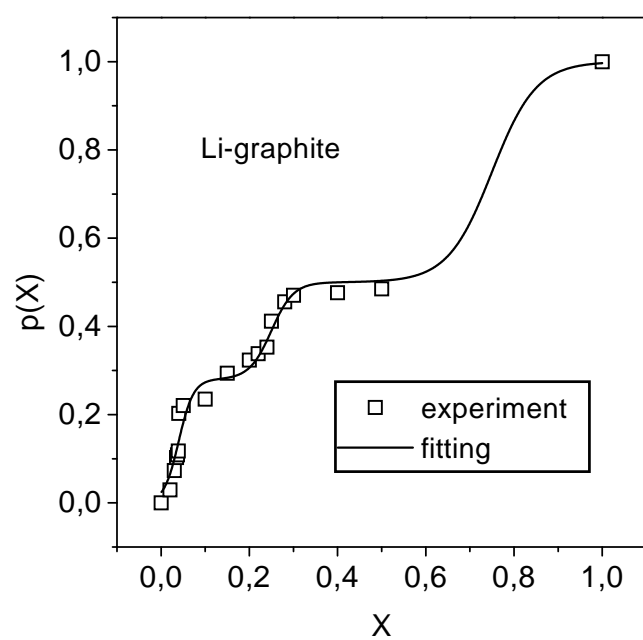


Figure 4

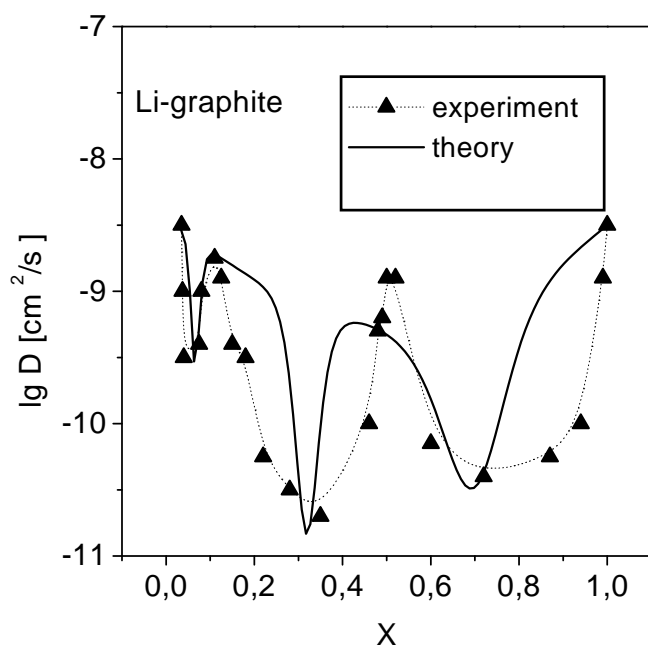


Figure 5